

## BACTERIA-CLAY INTERACTION: STRUCTURAL CHANGES IN SMECTITE INDUCED DURING BIOFILM FORMATION

ALEXANDRA ALIMOVA<sup>1</sup>, A. KATZ<sup>1</sup>, NICHOLAS STEINER<sup>2</sup>, ELIZABETH RUDOLPH<sup>2</sup>, HUI WEI<sup>3</sup>,  
JEFFREY C. STEINER<sup>2</sup>, AND PAUL GOTTLIEB<sup>3,\*</sup>

<sup>1</sup> Institute for Ultrafast Spectroscopy and Lasers, The City College of New York, 160 Convent Ave, New York, NY 10031, USA

<sup>2</sup> Department of Earth and Atmospheric Sciences, The City College of New York, 160 Convent Ave, New York, NY 10031, USA

<sup>3</sup> Sophie Davis School of Biomedical Education, The City College of New York, 160 Convent Ave, New York, NY 10031, USA

**Abstract**—Bacteria play an important role in determining the properties and behavior of clay minerals in natural environments and such interactions have great potential for creating stable biofilms and carbon storage sites in soils, but our knowledge of these interactions are far from complete. The purpose of this study was to understand better the effects of bacteria-generated biofilms on clay interlayer expansion. Mixtures of a colloidal, 2-water hectorite clay and *Pseudomonas syringae* in a minimal media suspension evolve into a polysaccharide-rich biofilm aggregate in time-series experiments lasting up to 1 week. X-ray diffraction analysis reveals that upon aggregation, the clay undergoes an initial interlayer contraction. Short-duration experiments, up to 72 h, result in a decrease in the  $d_{001}$  value from 1.50 to 1.26 nm. The initial interlayer contraction is followed in long-duration (up to 1 week) experiments by an expansion of the  $d_{001}$  value of 1.84 nm. The expansion is probably a result of large, biofilm-produced, polymeric molecules being emplaced in the interlayer site. The resultant organo-clay could provide a possible storage medium for carbon in a microbial colony setting.

**Key Words**—Bacteria-clay Interaction, Biofilms, Clay Interlayer, Smectite, Polysaccharides, *Pseudomonas syringae*.

### INTRODUCTION

Microorganisms are capable of creating and sustaining unique local environments on mineral surfaces (Fortin *et al.*, 1997; Fortin and Beveridge, 1997), within plant root systems (Dorioz *et al.*, 1993; Amellal *et al.*, 1998; Davey and O'Toole, 2000; Bloemberg and Lugtenberg, 2004), and in numerous fresh-water and marine environments (Ransom *et al.*, 1999). Organic matter has a strong effect on the chemical and physical properties of clays and sediments (Hedges and Oades, 1997; Stal, 2003; Gerbersdorf *et al.*, 2008). Within the confines of these environments, colonies of bacteria are reactive and influence the corrosion of metal surfaces (Pope *et al.*, 1984; Little *et al.*, 1991; Little *et al.*, 1997; Lee and Newman, 2003), contribute to the lithification of microbial mats (Chafetz and Buczynski, 1992; Reid *et al.*, 2000; Dupraz and Visscher, 2005; Baumgartner *et al.*, 2006), influence the erodability of sublittoral sediments (Sutherland *et al.*, 1998), as well as creating hazardous medical conditions (Costerton *et al.*, 1987). In soils, bacteria may activate chelated elements and influence nutrient transfer by solutions which surround plant roots (Bloemberg and Lugtenberg, 2004). These

nutrient transfers, which involve changes in local acidity and ion balance, can be strongly mitigated by interactions with clays.

The presence of smectite has been shown to be a key stimulus to the rapid growth of biofilms in a laboratory setting (Alimova *et al.*, 2006). In the marine environment, clay floccules protect organic matter from degradation (Ransom *et al.*, 1998, Curry *et al.*, 2007) and bacteria are known to disaggregate larger clay floccules (Jackson and Burd, 1998). Thus it is important to understand better the role of clays as important moderators of organic material exchange in natural systems.

The majority of floccule disaggregation processes are enabled by the production of biofilms. Biofilms consist of a matrix of bacteria cells and extracellular polymeric substances (EPS) with channels for providing water and nutrients to the cells. Extracellular components of biofilms can include polysaccharides, nucleic acids, and peptides. The clay aggregates embed non-soluble metal ions that result ultimately in the mineralization of epilithic biofilms (Konhauser *et al.*, 1994). These matrices can be synthesized in industrial prototype clay-biofilm reactors and have been shown to be of value for the extraction of nitrites and other contaminants (Zhang *et al.*, 2000). This complex of organic materials provides an important exchange system that may significantly affect the exchange of materials with the interstitial layers of clays. Polysaccharides are

\* E-mail address of corresponding author:

pgottl@med.cuny.edu

DOI: 10.1346/CCMN.2009.0570207

known to cause expansion in clays in cases without bacterial intervention (Ueshima and Tazaki, 2001, Darder and Ruiz-Hitzky, 2005) and assist in growing nontronite clay layers (Ueshima and Tazaki, 2001).

The purpose of this work was to determine the reaction of smectite and the production of biofilm in a system that involves a growing bacteria colony, *Pseudomonas syringae*, a representative soil-based plant pathogen. Pseudomonads are known to be prolific biofilm producers (O'Toole and Kolter, 1998). The smectite-bacteria interaction results in the formation of clay-bacteria aggregates associated within the biofilm. Whereas there are several seminal papers on the nature of the biofilms and their structure (*e.g.* Costerton *et al.*, 1995; Davey and O'Toole, 2000), there is very little information on the possible impact of the biofilm-aggregating bacteria on clay substrates. The present study uses X-ray diffraction (XRD) to measure changes in the (001) layering on passively settled, bio-reacted clay and to examine the likelihood of interlayer substitutions. A portion of the EPS output of the biofilm may be entrained in clay through exchange with water in the interlayer sites resulting in the formation of a unique type of organo-clay containing biofilm components.

## MATERIALS AND METHODS

### *Clay purification and size separation*

The smectite used in this study was hectorite, a lithium-based trioctahedral smectite (American Colloid Company, Arlington Heights, Illinois; commercial name: Hectalite; chemical formula:  $(\text{Ca},\text{Na})_{0.33}(\text{Mg}_{2.66},\text{Li}_{0.33})\text{Si}_4\text{O}_{10}(\text{F},\text{OH})_2$ ), which was first purified (organic contaminants removed) using Clorox bleach (5% sodium hypochlorite). Washing with Clorox is a standard method for the removal of organic materials from clay (Anderson, 1961; Mikutta *et al.*, 2005; Moore and Reynolds, 1997). The pH was adjusted to 9.0 by the addition of HCl. Two grams of clay were mixed with 200 mL of Clorox and incubated in a shaker for 40 min at 37°C. The organic-free clay was subjected to a triple wash with sterile, doubly distilled water to remove any Clorox residue. Next, the larger clay particles (>0.5 µm) and non-clay minerals were removed by centrifugation at 3600 rpm for 20 min. The pellet, containing the larger particles, was discarded. The supernatant containing the smaller clay particles (<0.5 µm) was autoclaved at 121°C and 15 psi for 40 min to destroy any possible bacterial contamination. The sterility of the hectorite suspension was tested by placing 100 µL on a Luria-Bertani (LB) agar plate and incubating for 2 days at 27°C. The LB media contained bacto-tryptone and bacto-yeast extract which together constitute an enriched media that supports the growth of many microorganisms, both bacterial and fungal (Difco, 1953). The absence of bacterial or fungal colonies after this time period was strong confirmation of the sterility of the clay.

### *Bacteria*

A single colony of *P. syringae* pv. *phaseolicola* HB10Y was transferred from an LB agar plate to 2 mL of minimal media. The minimal media consisted of: 50 mM of  $\text{NaH}_2\text{PO}_4$ , 20 mM of  $\text{KH}_2\text{PO}_4$ , 20 mM of  $\text{NH}_4\text{Cl}$ , 9 mM of  $\text{NaCl}$ , 0.01 mM of  $\text{CaCl}_2$ , 0.05 mM of  $\text{MgSO}_4$ , 0.4% of glucose, 4 µg/mL each of the amino-acids: proline, methionine, serine, and histidine, 40 µg/mL of sodium glutamate, and trace amounts of microelements Fe, Mo, Zn, Mn, Cu, Co, and B, at concentrations of ~0.1 µM. The bacteria, in log phase, were incubated in a shaker bath overnight at 27°C prior to mixing with the clay suspensions. Under these culture conditions, *P. syringae* were observed to begin forming aggregates within 3 h of mixing with smectite (Alimova *et al.*, 2006).

### *Clay-bacteria mix*

The *P. syringae*-clay suspensions were prepared by mixing 20 mL of media with 4 mL of the autoclaved hectorite and 500 µL of the overnight culture of *P. syringae*. The initial bacteria concentration for these experiments was ~10<sup>6</sup> colony forming units (CFU)/mL. Hectorite control suspensions were also prepared by mixing 4 mL of the autoclaved hectorite with 20 mL of minimal media but without *P. syringae*. The concentration of hectorite and nutrients in the controls are equal to that of the *P. syringae*-clay suspensions.

The *P. syringae*-clay suspensions were placed in sterile flasks and incubated for periods of up to 1 week at 27°C. After incubation, some of the samples were treated with Clorox to remove organic material, including bacteria cells and EPS. The free-floating bacteria and bacteria-clay aggregates were collected by centrifugation at 13,000 rpm with a Sorvall SS-34 rotor (~14,400 g) for 40 min. The supernatants were decanted and the pellets isolated. Some pellets were resuspended in 10 mL of Clorox at pH 9 in order to remove organic material. The suspensions were then incubated at 37°C for 1 h in a shaker bath and again centrifuged at 14,400 g for 20 min after which the pellets were washed three times with sterile, doubly distilled water. After the final wash, the pellets were re-suspended in 1 mL of water, transferred to Eppendorf tubes, and again centrifuged at 14,400 g for 30 min. The supernatant was discarded. The organic-free pellets and the clay-biofilm aggregate pellets were analyzed using XRD. The control specimens were centrifuged in the same manner as the bacteria-clay mixture but were not re-subjected to a Clorox bath because organic materials had previously been removed during the clay preparation and control-sample sterility was preserved during the experiment.

### *X-ray diffraction*

X-ray powder diffraction (XRD) patterns, acquired at different time periods following mixing with *P. syringae*, covered a 2θ angular range of 4–35° in either 0.005° or

0.01° steps using a PW3830 X-ray diffractometer (PANalytical Inc., Natick, Massachusetts). The integration time was 4 s per data point. The organic-free clay pellets were transferred to either glass slides or aluminum plates and air dried at room temperature (25°C) at ~40% humidity. The clays mounted on glass slides were mixed with 10  $\mu\text{L}$  of Brazilian talc in aqueous suspension and allowed to dry over several hours in order to produce and accentuate the preferred (001) orientation (Moore and Reynolds, 1997). Talc was used as an internal standard. After measuring the XRD pattern of the air-dried samples, they were solvated with ethylene glycol (EG) vapor at 60°C for 4 h. The shift in the basal reflection ( $d_{001}$ ) from 1.51 nm ( $5.87^{\circ}2\theta$ ) to 1.70 nm ( $5.2^{\circ}2\theta$ ) agreed with that predicted for hectorite expansion (Moore and Reynolds, 1997). The XRD patterns were also evaluated relative to theoretical smectite using the NEWMOD scattering algorithms (Version 2.1, <http://www.angelfire.com/md/newmod/index.html>). The water content was estimated by comparing XRD patterns with NEWMOD-generated spectra.

#### Scanning electron microscopy (SEM) and Energy dispersive X-ray analysis (EDX)

In preparation for SEM and EDX, 100  $\mu\text{L}$  of clay-*P. syringae* mixtures were taken from the flasks after 4 days of incubation. After conventional fixation with 8% glutaraldehyde, samples were filtered through polycarbonate membrane filters (0.2  $\mu\text{m}$  pore size) (Sterlitech Corporation, Kent, Washington) to remove residues of glutaraldehyde and minimal media. They were then dehydrated with ethanol gradient solutions and pure amyl acetate, followed by critical-point drying. The samples were carbon coated to improve conductivity.

The secondary electron emission images were acquired using a digital scanning electron microscope (DSM 940, Carl Zeiss, Germany). The EDX spectra were acquired using a liquid nitrogen-cooled energy dispersive X-ray detector (Princeton Gamma Tech, Princeton, New Jersey). The accelerating voltage was 15 kV.

## RESULTS AND DISCUSSION

Mixtures of *P. syringae* and clay began producing aggregates within 3 h. The aggregates eventually reached diameters of 10  $\mu\text{m}$  to 2 mm, consistent with previous results for several species of bacteria (Alimova *et al.*, 2006). In the absence of bacteria, aggregates failed to form during incubation periods of up to 1 week, demonstrating that the aggregates formed involved both the bacteria and the hectorite. A typical 20  $\mu\text{m}$  aggregate, formed after a 4-day interval, consisted of an agglomeration of biofilm (EPS and encased *P. syringae*) and clay (Figure 1a). Individual *P. syringae* cells (elongated cylinders) were observed both within and outside the EPS matrix. Unclear is whether the large number of *P. syringae* cells observed on the left side of Figure 1a are planktonic (isolated) cells, a component of the biofilm, or a localized area (or cluster) of independent cells. The Al-, Si-, and Fe-peaks in the EDX spectrum obtained using a 0.5  $\mu\text{m}$  beam (square shows the location in Figure 1a) demonstrate the presence of clay particles encased in the biofilm (Figure 1b).

The 001, 003, 004, and 005 basal reflections of the oriented hectorite control (Figure 2a) fit well with the theoretical NEWMOD model for a trioctahedral smectite with two water layers (Figure 2b). The water content estimated by this method was ~8.5 wt.%. The XRD

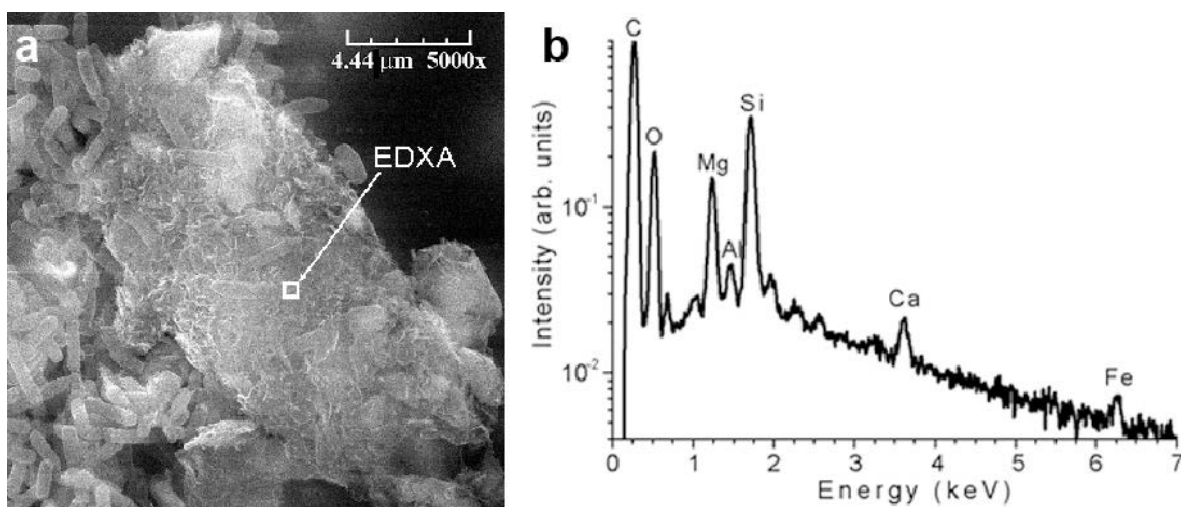


Figure 1. (a) Secondary electron emission image of a smectite-*P. syringae* aggregate after incubation for 4 days. *P. syringae* cells (cylindrical objects) are observed within the EPS matrix, and as possible planktonic cells (left side of image) outside of the EPS matrix. (b) EDX spectrum of the smectite-*P. syringae* aggregate acquired at the location shown in (a). EDX confirms that the biofilm aggregate contains clay particles.

pattern of hectorite immersed in minimal media (control) is identical to that of the clay not exposed to the minimal media, indicating minimal interaction between the clay and the media. Least-squares Lorentzian fitting of the (001) reflection yielded a peak position of  $5.87^\circ 2\theta$  ( $d_{001} = 1.51$  nm) and a full width at half maximum (FWHM) of  $0.97^\circ 2\theta$  (Figure 2c).

The evolution of the biofilm-clay reaction over time was monitored by acquiring the XRD pattern at 0, 1, 2, 4, 24, 72, and 168 h post-mixing (Figure 3). Within the first 2 h of mixing, little change was observed, as expected, because *P. syringae* only began to form biofilm-clay aggregates ~3 h after mixing (Alimova *et al.*, 2006). Upon formation of aggregates, the clay underwent an initial interlayer contraction and continued to contract for 3 days, shown by a progressive shift in the 001 peak to greater  $2\theta$  values. The 002 peak, which is not evident in the aggregates at early stages, began to appear at ~24 h, and in the present evaluation, increased in relative intensity in longer-duration experiments. Of

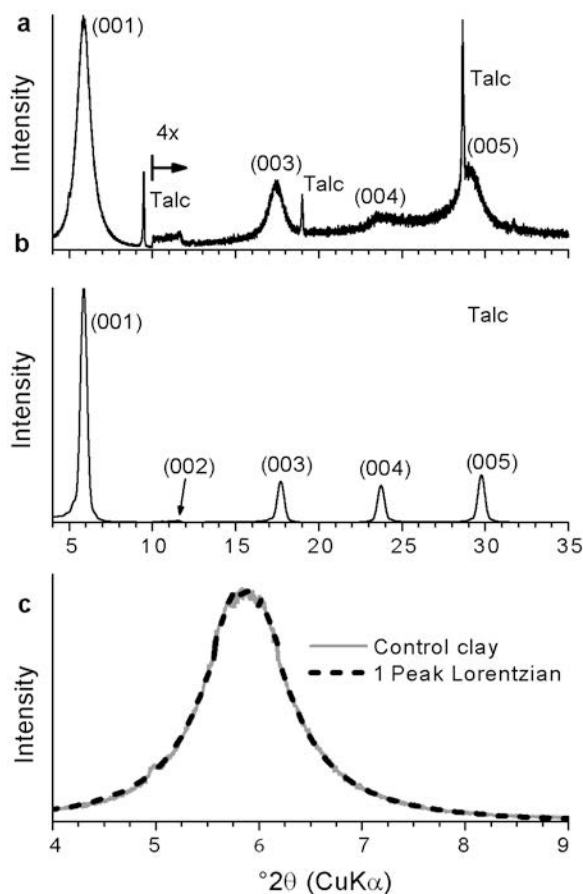


Figure 2. XRD spectra of (a) smectite control – no biofilm/bacteria contact; (b) NEWMOD-generated scattering approximation for hectorite with two interlayer water layers; and (c) 001 peak of smectite control and single-peak, least-squares Lorentzian fit;  $2\theta$  peak position is  $5.87^\circ$  and FWHM is  $0.97^\circ$ .

note is that the 002 peak was very weak in the NEWMOD-generated XRD pattern for hectorite with two interlayer water layers (Figure 2b). The 005 peak broadened and shifted toward smaller  $2\theta$  values for aggregation times  $>4$  h.

The pattern for the bio-reacted clay 1 week after mixing consists of a complex peak population and peaks that are generally broad (Figure 4a). The 001 peak shifted significantly toward smaller  $2\theta$  indicating expansion of the clay. The reaction also created additional peaks related to a varying degree of intercalation of organics into the clay. This inherently reflects a disequilibrium condition that is best approximated by finding solutions to the expansion condition using NEWMOD and selecting different crystal specifications. Two NEWMOD patterns, one for a smectite with two EG layers and the other for a mixture of one and two EG layers, approximated the peak positions (Figure 4a) reasonably well.

The 001 peak of the 1-week, bio-reacted hectorite can be represented as a composite of three individual 001 reflections. A 3-peak, least-squares Lorentzian fit (Figure 4b) of the 001 peak gave peaks at  $4.81^\circ 2\theta$  (FWHM:  $2.52^\circ 2\theta$ ),  $6.25^\circ 2\theta$  (FWHM:  $3.01^\circ 2\theta$ ), and  $8.73^\circ 2\theta$  (FWHM:  $2.28^\circ 2\theta$ ). The peak at  $4.81^\circ 2\theta$  represents a maximally expanded hectorite ( $d_{001} = 1.84$  nm). The  $6.25^\circ 2\theta$  peak is probably from a fraction of the hectorite that retained its original, non-expanded, water content. The  $8.73^\circ 2\theta$  'shoulder' is from the subset of clays which might have retained smaller molecules in the interlayer.

Removal of organic material by a Clorox wash of the clay-biofilm aggregates resulted in contraction of the bio-reacted hectorite, possibly related to removal of an interlayer polysaccharide component. Clorox washing

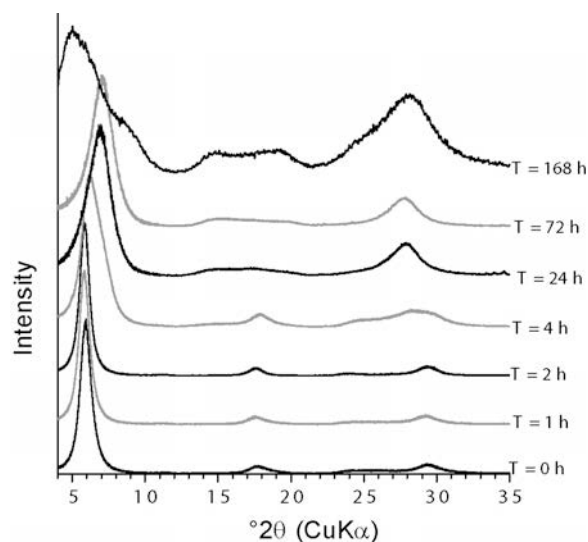


Figure 3. XRD spectra acquired immediately after mixing of smectite and *P. syringae* (T = 0) and at 1, 2, 4, 24, 72, and 168 h after mixing.



also contracted the EG-solvated hectorites (data not shown) in a manner similar to that observed for biofilm components. As can be observed in the XRD patterns of the Clorox washed clay (Figure 5a), the hectorite particles failed to return to a two-water layer interlayer configuration. The 001 peak was broader and shifted to a larger scattering angle. A two-peak Lorentzian fit of the 001 peak (Figure 5b) yielded peaks at  $6.09^{\circ}2\theta$  and  $6.83^{\circ}2\theta$  with FWHM values of  $1.29^{\circ}2\theta$  and  $0.74^{\circ}2\theta$ , respectively. NEWMOD approximations indicate that the clay was a mixture of one and two interlayer water layers with  $6.09^{\circ}2\theta$  peaks arising from grains with two interlayer water layers and the  $6.83^{\circ}2\theta$  peak arising from grains with one interlayer water layer. Washing the clay with Clorox removed the clay's organic matter, including all or a substantial proportion of the biofilm. This generated a reverse reaction that collapsed the clay to a 1- and 2-molecular water layer condition. This is consistent with the partial rehydration of a subset of the clay grains. The disappearance of the expanded peak at  $4.81^{\circ}2\theta$  and the  $8.73^{\circ}2\theta$  'contracted shoulder' after Clorox washing is strong evidence that their origins were organic interlayer material.

## CONCLUSIONS

Biofilm formation is accompanied by the secretion of molecules and macromolecules which remain in the

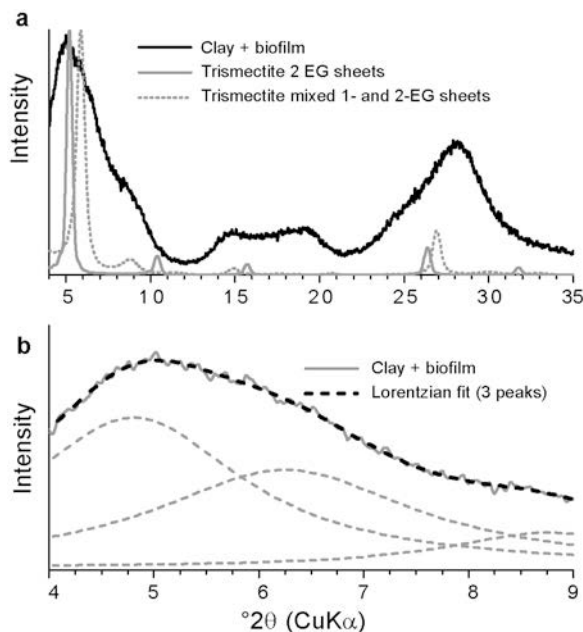


Figure 4. (a) XRD spectra of biofilm-reacted clay and NEWMOD-generated scattering spectra for hectorite with two ethylene glycol (EG) and mixed 1- and 2-EG interlayer layers. (b) 001 peak and three-peak, least-squares Lorentzian fit. The  $2\theta$  peak positions for the three components are:  $4.81^{\circ}$  (FWHM:  $2.52^{\circ}$ ),  $6.25^{\circ}$  (FWHM:  $3.01^{\circ}$ ) and  $8.73^{\circ}$  (FWHM:  $2.28^{\circ}$ ) and shown in (b) as dashed lines.

vicinity of the associated cells (Davey and O'Toole, 2000). Clay in suspension approximates the size of bacteria and, in the present case, facilitates biofilm formation (Alimova *et al.*, 2006). Initially, the biofilm-secreted molecules interact with the clay, replacing two interlayer water layers with small organic molecules. This results in a net contraction along the 001 basal plane of the clay. After longer time intervals, the clay expands, apparently responding to the replacement or addition of larger polymeric groups as more complex biofilm components are produced. The initial process of contraction, followed by the subsequent expansion, is illustrated schematically in Figure 6. The removal of organic material by treatment with Clorox results in a contraction of the clay as water is re-adsorbed, confirming that the interlayer material is organic in nature (one water layer is represented in Figure 6D). The evolution of biofilm and its organic component is a causal agent in the production of organo-clays.

The XRD analysis demonstrates that biofilm has a profound effect on the physical structure of the clay, resulting in the expansion and contraction steps observed, strongly suggesting that cell-derived organic compounds readily transit in and out of the clay structure and influence the complex communication or signaling steps (quorum sensing) that are widely discussed as important features of the evolution of biofilms in natural bacterial colonies.

Evidence suggests further that the interactions between bacteria and clay particles are beneficial to

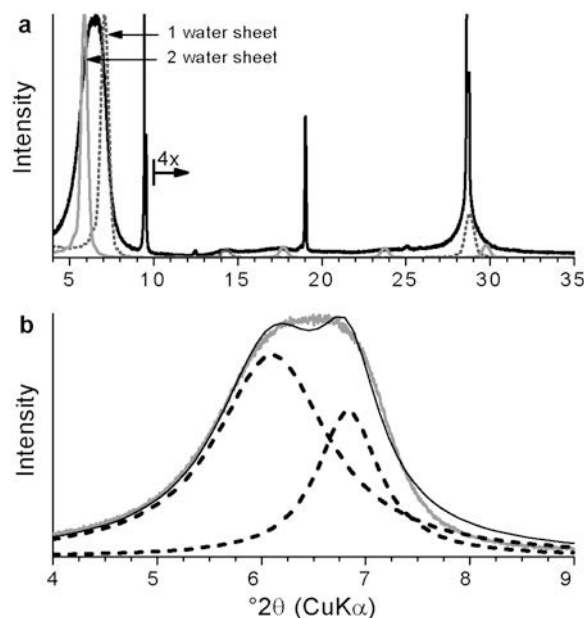


Figure 5. (a) Biofilm-reacted clay after removal of organic material by Clorox washing, and NEWMOD-generated scattering patterns for a hectorite with one and two interlayer water layers. (b) 001 peak and two-peak, least-squares Lorentzian fit to the 001 peak.

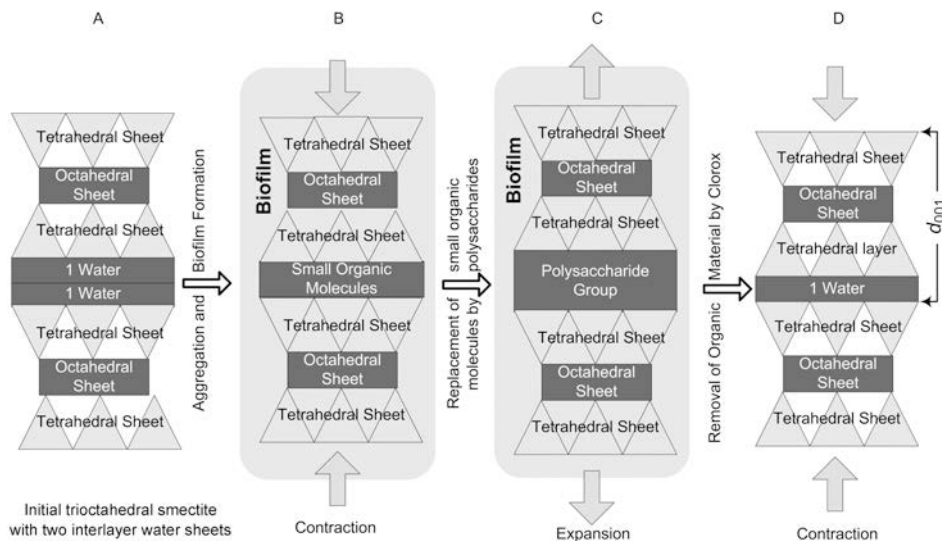


Figure 6. Time evolution of the smectite-biofilm interaction. Hectorite with two interlayer water layers (A) initially contracts during biofilm formation as small organic molecules secrete into the interlayer (B). Eventually, the secretion of polysaccharides into the interlayer expands the clay (C). Subsequent removal of organic material by Clorox contracts the clay (D) as water is partially reabsorbed back into the interlayer.

bacteria. For example, the ability of microbes to survive long-range transport during dust storms (McCarthy, 2001; Taylor, 2002; Griffin *et al.*, 2001; Griffin *et al.*, 2003; Ruiz-Conde *et al.*, 1997) would indicate that adherence to dust clay particles may protect bacteria against dehydration and ultraviolet light. Studies have shown that clay minerals protect DNA from damage due to UV exposure (Bitton *et al.*, 1972; Scappini *et al.*, 2004). Clays can also act as a source of minerals and cations (*e.g.*  $Mg^{2+}$ ,  $Ca^{2+}$ ,  $Fe^{3+}$ ,  $Li^+$ ). Bacteria are known to extract Fe(III) from clays (Stucki *et al.*, 1987; Kostka *et al.*, 2002; Stucki and Kostka, 2006). Iron reduction by bacteria impacts the surface chemistry of the clays, reducing swelling pressure and decreasing surface area (Kostka *et al.*, 1999). This decrease in the ability of hectorites to swell results in a collapse of the clay

interlayer (Stucki *et al.*, 2000). On the other hand, aluminum toxicity may inhibit some species of bacteria from adhering to minerals with extractable aluminum (Bulson *et al.*, 1984; Pina and Cervantes, 1996). The role of Al- and Fe-rich silicates in the attachment of microbial cells to mineral surfaces has been explored (Roberts, 2004). The large surface area of clay particles promotes surface adhesion and clumping of bacteria (Vieira *et al.*, 2001). Clay sediments have been shown to enhance survival rates for several different species of enteric bacteria in fresh water (Burton *et al.*, 1987). Recent work on the promotion of biofilm formation by clay particles demonstrates that the smectite-bacteria interaction increases bacteria viability for several different species (Alimova *et al.*, 2006).

The clay interlayer contraction observed could be the result of the incorporation of small organic molecules (*e.g.* amino acids, nucleic acids, monosaccharides) in the interlayer space. Contraction in vermiculites, caused by aliphatic amides, has also been observed (Ruiz-Conde *et al.*, 1997).

The initial contraction period is proposed to have eventually been replaced by an interlayer expansion related to the production of polysaccharides in the biofilm matrix. These large polymeric species are thus exuded into the clay interlayer during later stages of the reaction series. The contraction and expansion cycle is observable as changes in the  $2\theta$  position of the 001 peaks as a function of aggregation time (Figure 7). Ethylene glycol solvation results in the characteristic negative shift in  $2\theta$  (spectra not shown), indicating expansion of the interlayer, and confirming that the clay aggregates remain smectitic.

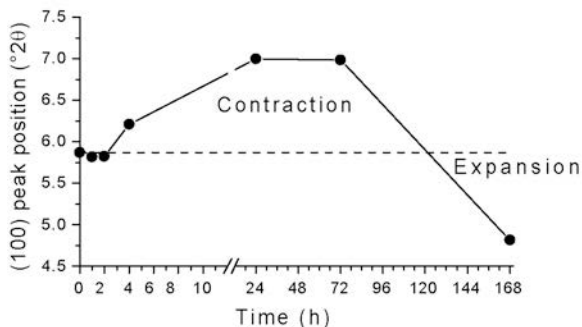


Figure 7. Position of 001 maxima at different incubation times for *P. syringae*-smectite clay mixtures. Aggregation begins at ~3 h.

## ACKNOWLEDGMENTS

This work was supported in part by a NASA URC—The Center for Optical Sensing and Imaging at The City College of New York, grant NCC-1-03009; and the National Institutes of Health, grant RCM1 G12RR-03060. The authors also acknowledge support provided by the NOAA Center for Cooperative Remote Sensing Science and Technology, grant NA17AE1625.

## REFERENCES

- Alimova, A., Roberts, M., Katz, A., Rudolph, E., Steiner, J. C., Alfano, R.R., and Gottlieb, P. (2006) Effects of smectite clay on biofilm formation by microorganisms. *Biofilms*, **3**, 47–54.
- Amellal, N., Burtin, G., Bartoli, F., and Heulin, T. (1998) Colonization of wheat roots by an exopolysaccharide-producing *Pantoea agglomerans* strain and its effect on rhizosphere soil aggregation. *Applied and Environmental Microbiology*, **64**, 3740–3747.
- Anderson, J.U. (1961) An improved pretreatment for mineralogical analysis of samples containing organic matter. *Clays and Clay Minerals*, **10**, 380–388.
- Baumgartner, L.K., Reid, R.P., Dupraz, C., Decho, A.W., Buckley, D.H., Spear, J.R., Przekop, P.K.M., and Visscher, P.T. (2006) Sulfate reducing bacteria in microbial mats: Changing paradigms, new discoveries. *Sedimentary Geology*, **185**, 131–145.
- Bitton, G., Henis, Y., and Lahav, N. (1972) Effect of several clay minerals and humic acid on the survival of *Klebsiella aerogenes* exposed to ultraviolet irradiation. *Applied Microbiology*, **23**, 870–874.
- Bloemberg, G.V. and Lugtenberg, B.J.J. (2004) *Bacterial Biofilms on Plants: Relevance and Phenotypic Aspects*. ASM Press, Washington, D.C.
- Bulson, P.C., Johnstone, D.L., Gibbons, H.L., and Funk, W.H. (1984) Removal and inactivation of bacteria during alum treatment of a lake. *Applied and Environmental Microbiology*, **48**, 425–430.
- Burton, G.A., Jr., Gunnison, D., and Lanza, G.R. (1987) Survival of pathogenic bacteria in various freshwater sediments. *Applied and Environmental Microbiology*, **53**, 633–638.
- Chafetz, H.S. and Buczynski, C. (1992) Bacterially induced lithification of microbial mats. *Palaios*, **7**, 277–293.
- Costerton, J.W., Cheng, K.J., Geesey, G.G., Ladd, T.I., Nickel, J.C., Dasgupta, M., and Marrie, T.J. (1987) Bacterial biofilms in nature and disease. *Annual Review of Microbiology*, **41**, 435–464.
- Costerton, J.W., Lewandowski, Z., Caldwell, D.E., Korber, D.R., and Lappin-Scott, H.M. (1995) Microbial biofilms. *Annual Review of Microbiology*, **49**, 711–745.
- Curry, K.J., Bennett, R.H., Mayer, L.M., Curry, A., Abril, M., Biesiot, P.M., and Hulbert, M.H. (2007) Direct visualization of clay microfabric signatures driving organic matter preservation in fine-grained sediment. *Geochimica et Cosmochimica Acta*, **71**, 1709–1720.
- Darder, M. and Ruiz-Hitzky, E. (2005) Caramel–clay nanocomposites. *Journal of Materials Chemistry*, **15**, 3913–3918.
- Davey, M.E. and O’toole, G.A. (2000) Microbial biofilms: from ecology to molecular genetics. *Microbiology and Molecular Biology Reviews*, **64**, 847–867.
- Difco (1953) *Manual of Dehydrated Culture Media and Reagents for Microbiological and Clinical Laboratory Procedures Laboratories*. Difco Laboratories, Detroit, USA
- Doriz, J.M., Robert, M., and Chenu, C. (1993) The role of roots, fungi and bacteria on clay particle organization. An experimental approach. *Geoderma*, **56**, 179–194.
- Dupraz, C. and Visscher, P.T. (2005) Microbial lithification in marine stromatolites and hypersaline mats. *Trends in Microbiology*, **13**, 429–438.
- Fortin, D. and Beveridge, T.J. (1997) Microbial sulfate reduction within sulfidic mine tailings: formation of diagenetic Fe-sulfides. *Geomicrobiology Journal*, **14**, 1–21.
- Fortin, D., Ferris, F.G., and Beveridge, T.J. (1997) Surface-mediated mineral development by bacteria. Pp. 161–180 in: *Geomicrobiology: Interactions Between Microbes and Minerals* (J.F. Banfield and K.H. Nealson, editors). Reviews in Mineralogy, **35**, Mineralogical Society of America, Washington, D.C.
- Gerbersdorf, S.U., Jancke, T., Westrich, B., and Paterson, D.M. (2008) Microbial stabilization of riverine sediments by extracellular polymeric substances. *Geobiology*, **6**, 57–69.
- Griffin, D., Garrison, V., Herman, J., and Shinn, E. (2001) African desert dust in the Caribbean atmosphere: Microbiology and public health. *Aerobiologia*, **17**, 203–213.
- Griffin, D.W., Kellogg, C.A., Garrison, V.H., Lisle, J.T., Borden, T.C., and Shinn, E.A. (2003) Atmospheric microbiology in the northern Caribbean during African dust events. *Aerobiologia*, **19**, 143–157.
- Hedges, J.I. and Oades, J.M. (1997) Comparative organic geochemistries of soils and marine sediments. *Organic Geochemistry*, **27**, 319–361.
- Jackson, G.A. and Burd, A.B. (1998) Aggregation in the marine environment. *Environmental Science and Technology*, **32**, 2805–2814.
- Konhauser, K.O., Schultze-Lam, S., Ferris, F.G., Fyfe, W.S., Longstaffe, F.J., and Beveridge, T.J. (1994) Mineral precipitation by epilithic biofilms in the Speed River, Ontario, Canada. *Applied and Environmental Microbiology*, **60**, 549–553.
- Kostka, J.E., Wu, J., Nealson, K.H., and Stucki, J.W. (1999) The impact of structural Fe(III) reduction by bacteria on the surface chemistry of smectite clay minerals. *Geochimica et Cosmochimica Acta*, **63**, 3705–3713.
- Kostka, J.E., Dalton, D.D., Skelton, H., Dollhopf, S., and Stucki, J.W. (2002) Growth of Iron(III)-reducing bacteria on clay minerals as the sole electron acceptor and comparison of growth yields on a variety of oxidized iron forms. *Applied and Environmental Microbiology*, **68**, 6256–6262.
- Lee, A.K. and Newman, D.K. (2003) Microbial iron respiration: impacts on corrosion processes. *Applied Microbiology and Biotechnology*, **62**, 134–139.
- Little, B.J., Wagner, P.A., and Mansfeld, F. (1991) Microbiologically influenced corrosion of metals and alloys. *International Materials Reviews*, **36**, 253–272.
- Little, B.J., Wagner, P.A., and Lewandowski, Z. (1997) Spatial relationships between bacteria and mineral surfaces. Pp. 123–155 in: *Geomicrobiology – Interactions Between Microbes and Minerals* (J.F. Banfield and K.H. Nealson, editors). Reviews in Mineralogy, **35**, Mineralogical Society of America, Washington D.C.
- McCarthy, M. (2001) Dust clouds implicated in spread of infection. *The Lancet*, **358**, 478.
- Mikutta, R., Kleber, M., Kaiser, K., and Jahn, R. (2005) Review: organic matter removal from soils using hydrogen peroxide, sodium hypochlorite, and disodium peroxodisulfate. *Soil Science Society of America Journal*, **69**, 120–135.
- Moore, D. and Reynolds, R.C., Jr. (1997) *X-ray Diffraction and the Identification and Analysis of Clay Minerals*, Oxford University Press, New York.
- O’Toole, G.A. and Kolter, R. (1998) Flagellar and twitching motility are necessary for *Pseudomonas aeruginosa* biofilm development. *Molecular Microbiology*, **30**, 295–304.
- Pina, R.G. and Cervantes, C. (1996) Microbial interactions

- with aluminium. *Biometals*, **9**, 311–316.
- Pope, D., Duquette, D., Wayner, P.C., and Johannes, A.H. (1984) *Microbiologically Influenced Corrosion: A State of the Art Review*. Columbus, OH, Materials Technology Institute of Chemical Process Industries.
- Ransom, B., Kim, D., Kastner, M., and Wainwright, S. (1998) Organic matter preservation on continental slopes: importance of mineralogy and surface area. *Geochimica et Cosmochimica Acta*, **62**, 1329–1345.
- Ransom, B., Bennett, R.H., Baerwald, R., Hulbert, M.H., and Burkett, P.-J. (1999) In situ conditions and interactions between microbes and minerals in fine-grained marine sediments; a TEM microfabric perspective. *American Mineralogist*, **84**, 183–192.
- Reid, R.P., Visscher, P.T., Decho, A.W., Stolz, J.F., Bebout, B.M., Dupraz, C., Macintyre, I.G., Paerl, H.W., Pinckney, J.L., Prufert-Bebout, L., Stegge, T.F., and Desmarais, D.J. (2000) The role of microbes in accretion, lamination and early lithification of modern marine stromatolites. *Nature*, **406**, 989–992.
- Roberts, J.A. (2004) Inhibition and enhancement of microbial surface colonization: the role of silicate composition. *Chemical Geology*, **212**, 313–327.
- Ruiz-Conde, A., Ruiz-Amil, A., Perez-Rodriguez, J.L., Sanchez-Soto, P.J., and De La Cruz, F.A. (1997) Interaction of vermiculite with aliphatic amides (formamide, acetamide and propionamide): formation and study of interstratified phases in the transformation of Mg- to NH<sub>4</sub>-vermiculite. *Clays and Clay Minerals*, **45**, 311–326.
- Scappini, F., Casadei, F., Zamboni, R., Franchi, M., Gallori, E., and Monti, S. (2004) Protective effect of clay minerals on adsorbed nucleic acid against UV radiation: possible role in the origin of life. *International Journal of Astrobiology*, **3**, 17–19.
- Stal, L.J. (2003) Microphytobenthos, their extracellular polymeric substances, and the morphogenesis of intertidal sediments. *Geomicrobiology Journal*, **20**, 463–478.
- Stucki, J.W. and Kostka, J.E. (2006) Microbial reduction of iron in smectite. *Comptes Rendus Geosciences*, **338**, 468–475.
- Stucki, J.W., Komadel, P., and Wilkinson, H.T. (1987) Microbial reduction of structural iron(III) in smectites. *Soil Science Society of America Journal*, **51**, 1663–1665.
- Stucki, J.W., Jun, W., Gan, H., Komadel, P., and Banin, A. (2000) Effects of iron oxidation state and organic cations on dioctahedral smectite hydration. *Clays and Clay Minerals*, **48**, 290–298.
- Sutherland, T.F., Amos, C.L., and Grant, J. (1998) The effect of buoyant biofilms on the erodibility of sublittoral sediments of a temperate microtidal estuary. *Limnology and Oceanography*, **43**, 225–235.
- Taylor, D.A. (2002) DUST in the WIND. *Environmental Health Perspectives*, **110**, A80–87.
- Ueshima, M. and Tazaki, K. (2001) Possible role of microbial polysaccharides in nontronite formation. *Clays and Clay Minerals*, **49**, 292–299.
- Vieira, M.J., Pacheco, A.P., Pinho, I.A., and Melo, L.F. (2001) The effect of clay particles on the activity of suspended autotrophic nitrifying bacteria and on the performance of an air-lift reactor. *Environmental Technology*, **22**, 123–135.
- Zhang, S.-Y., Wang, J.-S., Jiang, Z.-C., and Chen, M.-X. (2000) Nitrite accumulation in an Attapulgas clay biofilm reactor by fulvic acids. *Bioresource Technology*, **73**, 91–93.

(Received 16 September 2008; revised 12 December 2008; Ms. 0198; A.E. L. Williams)